Physiologia Plantarum
An International Journal for Plant Biology

Physiologia Plantarum 149: 286–295. 2013

Willow seedlings from photooxidized seeds accelerate cotyledon death and anticipate first leaf emergence: a histological and biochemical study following germination

Gonzalo Roqueiro[a,b], Fabio Causin[c], Carolina Olle-Resa[c], Horacio Maroder[b] and Sara Maldonado[c,*]

[a]Estación Experimental Agropecuaria San Juan, INTA, J5427ZAA, Pocito, San Juan, Argentina
[b]Departamento de Ciencias Básicas, Universidad Nacional de Luján, 6700, Luján, Argentina
[c]Departamento de Biodiversidad y Biología Experimental, Facultad de Ciencias Exactas y Naturales, Universidad de Buenos Aires, C1428EGA, Buenos Aires, Argentina

Correspondence
*Corresponding author,
e-mail: saram@bg.fcen.uba.ar

Received 22 December 2012;
revised 28 February 2013

doi:10.1111/ppl.12048

In willow seeds, photooxidative damage is mainly restricted to the outer cotyledonary tissues, significantly reducing normal germination. Here we analyzed the damage generated in cotyledonary tissues and investigated whether the increase in reactive oxygen species (ROS) generation in seedlings from photooxidized seeds can affect the morphogenetic capacity of the shoot apical meristem. Seeds were photooxidized under different light intensities and the evolution of the damage during seedling growth was studied by light and transmission electron microscopies. The level of lipid peroxidation and changes in antioxidant capacity were measured following the time course of superoxide dismutase, catalase, ascorbate peroxidase and guaiacol peroxidase enzyme activities, and the effect of photooxidative stress on the genesis of new leaf primordia and lateral roots was examined. Early and active endocytosis and autophagy, changes in chloroplast morphology, as well as the accumulation and diffusion of ROS all play important roles in the early cell death observed in cotyledonary tissues. Following germination, seedlings from photooxidized seeds anticipated the emergence of first leaves, which complemented the altered functionality of the damaged cotyledons.

Introduction

In nature, the seeds of different willow species show a rapid loss of viability and a decrease in germination to nearly zero a few days after shedding (Teng and Yu 1948, Arya et al. 1988). Hong et al. (1996), compiling data from various authors, classified 28 species of *Salix* as orthodox, excluding *S. caprea* which they consider intermediate. More recently, Popova et al. (2012) demonstrate that fresh *S. caprea* seeds tolerate desiccation up to 8.5–9.6 moisture content without any noticeable loss in viability. Additionally, Maroder et al. (2000) and Roqueiro et al. (2010, 2012) add three species, i.e. *S. alba* L., *S. matsudana* Koidz. and *Salix nigra* L., to Hong et al.'s group of short-lived orthodox seeds.

According to Maroder et al. (2003), the mature seeds of most willow species are exendospermous and contain a straight and chlorophyllous embryo covered by a thin seed coat. Subcellular studies in the cells of cotyledons and hypocotyl-radicle axis tissues have revealed the extensive presence of protein bodies with

Abbreviations – APX, ascorbate peroxidase; CAT, catalase; DAB, 3,3′-diaminobenzidine-HCl; DAS, days after sowing; dwb, dry weight basis; HSD, honestly significant difference; LM, light microscopy; MDA, malondialdehyde; NBT, nitro-blue tetrazolium chloride; NG, normal germination; PCD, programmed cell death; POX, guaiacol peroxidase; RH, relative humidity; ROS, reactive oxygen species; SOD, superoxide dismutase; TEM, transmission electron microscopy; TG, total germination.

globoid crystals, lipid bodies and chloroplasts, the latter having well-developed grana and, occasionally, starch grains in the stroma. In apical meristem cells, plastids are not organized in grana and contain deposits of phytoferritin in their stroma. Mature willow embryos are typically characterized by the presence of cells with a large central vacuole and a narrow peripheral band of cytoplasm, with scarce protein bodies, in the subdermal layers of cotyledons and the axis.

The presence of chlorophyll is not a common trait among mature seeds. Chloroplasts and chlorophyll have been found in the embryonic tissues of mature seeds of *Nelumbo nucifera* (Zhukova and Yakovlev 1966), *Kochia childsii* (Marin and Dengler 1972), *Acer pseudoplatanus* (Pinfield et al. 1973), *Avicennia marina* (Farrant et al. 1992, 1997), *Ekebergia capensis* (Pammenter et al. 1998) and *Pisum sativum* (Werker 1997). *Acer pseudoplatanus* (Daws et al. 2006) and *P. sativum* (Leprince 2003) are orthodox, while *A. marina* and *E. capensis* are considered recalcitrant (Pinfield et al. 1973, Farrant et al. 1992, Pammenter et al. 1998). Furthermore, *K. childsii*'s storage behavior is unknown and *N. nucifera*'s seeds are long-living. Thus, the presence of chloroplasts in mature embryos does not appear to be correlated with the seed's storage behavior.

The chlorophyllous seeds of willow are highly susceptible to photooxidation as compared to other (chlorophyllous or non-chlorophyllous) seeds with orthodox behavior. According to Roqueiro et al. (2010, 2012), the presence of chloroplasts with well-developed grana increases the risk of oxidative damage when seeds are stored in the presence of light. In fact, the thylakoid membranes are the first target of the photooxidative process, and light and oxygen play an important role in the generation of reactive oxygen species (ROS), causing lipid peroxidation, protein oxidation and a decrease in both pigment content and antioxidant enzyme activities. As a consequence, a marked decrease in seed vigor occurs, as indicated by a reduction in normal germination (NG) percentage and an increase in mean germination time.

Under low light intensity photooxidative damage is mainly restricted to the outer cotyledonary tissues, so that seed germination is not inhibited. However, the question remains whether seedling growth and/or development can proceed in photooxidized seeds once germination has taken place. In this study, we were particularly interested in whether the damage generated in cotyledons is reversible and whether the increase in ROS generation in damaged cotyledons can affect the morphogenetic capacity of the shoot apical meristem.

To answer these questions, we used seeds of one of the willow species (*S. nigra* L.) that had been photooxidized under two different light intensities, and examined the evolution of photooxidative damage during seedling growth both at tissular and cellular levels. We mainly analyzed the effects of light on cell ultrastructure with special emphasis on chloroplast morphology and function, and the production and localization of ROS at the tissue level. We also monitored the level of lipid peroxidation as an indicator of molecular damage, measured changes in key antioxidant enzyme activities and examined the effect of photooxidative stress on the genesis of new leaf primordia and lateral roots.

Material and methods

Plant material

Seeds from *S. nigra* L. trees were collected during mid-November 2006 in the Delta area of the province of Buenos Aires, Argentina. Seeds were manipulated under dim light to reduce the eventual generation of ROS, and stored at -80°C according to Maroder et al. (2000). Water content was estimated to be around 8%, expressed in dry weight basis (dwb).

Photooxidation treatments

Seeds were photooxidized at two light intensities, according to the experimental procedure described by Roqueiro et al. (2012). In short, seeds were stored for 3 days in the dark or under cool-white fluorescent light at either 2 (low light intensity) or 10 (high light intensity) μmol m^{-2} s^{-1}, at 25°C and 45% relative humidity (RH) (over K_2CO_3 saturated solution), in order to stabilize water content at 9–10% (dwb). The lower intensity corresponds to the average photosynthetic photon flux density measured on ground surface, where seeds fall after being scattered under a dense canopy; the higher intensity corresponds to the maximum intensity which barely affects total germination (TG), but significantly reduces NG percent (Roqueiro et al. 2012). The treatments were carried out in a SANYO MIR-153 Cooled Incubator. Control seeds corresponded to those stored at -80°C.

Germination test and morphogenetic analysis

Seeds were tested for germination over three pieces of filter paper moistened with 3.5 cm^3 distilled-deionized water in 6-cm diameter Petri dishes at $25 \pm 1^{\circ}$C and under a 16 h fluorescent light photoperiod for 24 and 48 h. Four replicates of 30 seeds were used for each treatment. Following germination, the development of lateral roots and leaves was examined on the 3rd, 7th, 14th and 21st days after sowing (DAS).

Light microscopy and transmission electron microscopy

Microscopic studies were carried out on 3-, 7-, 14- and 21-day-old seedlings, by fixing cotyledons from different treatments in 2.5% glutaraldehyde in 0.1 *M* phosphate buffer, pH 6.8, at 4°C, for 90 min. They were then post-fixed in 1% OsO_4 in the same buffer for 90 min, dehydrated in a graded ethanol series and embedded in Spurr's resin (Sigma-Aldrich, St. Louis, MO).

For light microscopy (LM), semi-thin sections were mounted on glass slides, stained in 0.1% toluidine blue O (Sigma-Aldrich T3260-5G) in aqueous solution and examined in an Axioskope 2 microscope (Carl Zeiss, Jena, Germany). Images were obtained using a Cannon EOS 1000 D camera (Tokyo, Japan) and processed using Axiovision 4.8.2 software (Carl Zeiss).

For transmission electron microscopy (TEM), ultra-thin sections were mounted on grids coated with Formvar, and then carbon, stained in uranyl acetate (EMS 22400) followed by lead citrate (EMS 18510), and examined in a Zeiss M109 transmission electron microscope.

H_2O_2 in situ detection

The method used for in situ H_2O_2 detection was based on the generation of a brown precipitate in the presence of 3,3′-diaminobenzidine-HCl (DAB) (Romero-Puertas et al. 2004). For each treatment, four replicates of 30 seedlings were soaked in a 0.1% DAB solution. After 1 h of incubation, the seedlings were rinsed with distilled water and bleached overnight with 80% ethanol. The development of a brown precipitate in the cotyledonal tissues was observed under a Stemi 200-C Carl Zeiss stereomicroscope (Göttingen, Germany), equipped with a Sony Cyber-Shot DSC-W570 Digital Camera 6 X (Tokyo, Japan).

$O_2^{\bullet-}$ in situ detection

The presence of $O_2^{\bullet-}$ was determined by the formation of a blue precipitate in the presence of nitro-blue tetrazolium chloride (NBT) (Romero-Puertas et al. 2004). For each treatment, four replicates of 30 seedlings were incubated for 1 h in a 0.1% NBT water solution, rinsed with distilled water and bleached overnight in 80% ethanol. As a negative control, seedlings were incubated for 30 min in a 12 m*M* $MnCl_2$ solution, (an $O_2^{\bullet-}$ scavenger) prior to NBT staining.

Malondialdehyde

Malondialdehyde (MDA) formation in cotyledonary tissues was determined according to Vavilin et al. (1998). For each treatment, four replicates of 30 cotyledons (approximately 150 mg) were homogenized with 1.5 ml reagent containing 0.3% thiobarbituric acid, 4% trichloroacetic acid, 0.01% butylatehydroxytoluene and heated for 30 min at 95°C. Samples were cooled to room temperature and centrifuged at maximum speed to obtain a clear supernatant. MDA concentration was determined using Hodges et al.'s (1997) equation.

Antioxidant enzymes

For each treatment, four replicates of 30 cotyledons (approximately 150 mg) were homogenized with 1.5 ml of potassium phosphate buffer (pH 7.8) containing 1 m*M* ethylenediaminetetraacetic acid, 1% (w/v) polyvinylpyrrolidone, 0.5 m*M* phenylmethylsulphonyl fluoride and 0.2 m*M* benzamidine. The homogenate was centrifuged at 16 000 *g* (4°C) for 30 min, and the supernatant obtained used for enzyme activity assays. Enzyme activity of superoxide dismutase (SOD) (EC 1.15.1.1), ascorbate peroxidase (APX) (EC 1.11.1.11), guaiacol peroxidase (POX) (EC 1.11.1.7) and catalase (CAT) (EC 1.11.1.6) was evaluated according to Beauchamp and Fridovich (1971), Nakano and Asada (1987), Prochazkova et al. (2001) and Aeibi (1984), respectively.

Statistical analysis

When applicable, data were analyzed by one-way ANOVA (Statistics Calculators version 3.0), and differences among treatments were determined following Tukey honestly significant difference (HSD) post hoc test, at $\alpha \leq 0.05$. Values correspond to means ± SD.

Results

Germination and morphogenesis

Under the experimental conditions applied in this study, photooxidation treatments did not alter the percentage of TG but markedly affected NG as well as seedling survival rates (Table 1). Germination was considered normal if the seedling developed a hypocotyl, root and cotyledons, and stood erect. Seedlings not meeting these criteria were classified as abnormal; likewise, seedlings with cotyledons exhibiting incipient chlorosis and/or necrotic areas were also considered as abnormal. TG was calculated as the sum of normal and abnormal germination. The types of damage most commonly observed in photooxidized seeds were: (1) smaller seedlings; (2) underdeveloped radicles and (3)

Table 1. TG and NG percentages at 7 DAS, in control seeds and seeds photooxidized at 2 and 10 μmol m^{-2} s^{-1}. Values for treatments with the same letters are not significantly different ($P < 0.05$).

Seed treatments	TG	NG
Control	100% a	98 ± 4% a
Photooxidation under 2 μmol m^{-2} s^{-1}	99 ± 2% a	57 ± 4% b
Photooxidation under 10 μmol m^{-2} s^{-1}	99 ± 2% a	16 ± 7% c

Table 2. ANOVA of percent of viable seedlings and percent viable seedlings with first leaves at different DAS, from control seeds and seeds photooxidized at 2 and 10 μmol m^{-2} s^{-1}.

DAS		d.f.	F-value	*P*-value
7	% Viable seedlings	2	1.33	0.29
	% Viable seedlings with first leaves		n.d	
14	% Viable seedlings	2	153.60	<0.01
	% Viable seedlings with first leaves	2	25.28	<0.01
21	% Viable seedlings	2	53.62	<0.01
	% Viable seedlings with first leaves	2	29.95	<0.01

pale-green cotyledons with necrotic areas in abaxial surfaces and borders. All of these effects increased with light intensity and were taken into account when determining NG.

Cotyledons expanded and reached their final size during the first 3–7 days following germination, although there were clear differences between the control seedlings and those derived from photooxidized seeds (see below).

Seedlings with first leaves could be found at 14 DAS in all treatments (Fig. 1A–C), but the percentage was significantly higher in those derived from both photooxidation treatments (Table 2). A similar trend was observed at 21 DAS. By this time, the development of the first leaves clearly differed among treatments as their relative size was about 1.7–3.8 folds higher than the control, in seedlings from the 2 and 10 μmol m^{-2} s^{-1} photooxidation treatments, respectively (Fig. 4B).

The first lateral roots emerged under the basal region of the hypocotyls (Fig. 1B–C), where the first root hairs usually sprout (Pólya 1961).The percentage of seedlings with lateral roots increased with time and did not significantly differ among treatments (data not shown).

Histological and cellular analysis of cotyledons

Figures 2 and 3 show sections of cotyledon tissues from the control and the two light treatments as analyzed by LM and TEM, respectively, at 3 DAS. During germination, mesophyll cells in control seedlings consumed storage reserves, generating vacuolated cells with

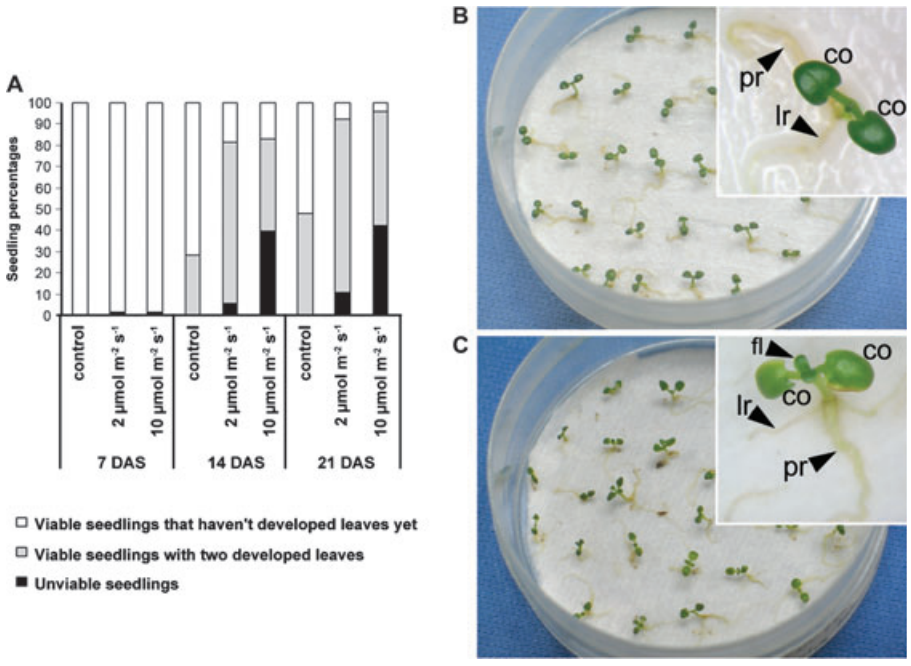

Fig. 1. Development of leaves in seedlings derived from non-photooxidized (control) seeds and seeds photooxidized at 2 or 10 μmol m^{-2} s^{-1}, at 7, 14 and 21 DAS. Bar values are means of four replicates of 30 seedlings. (B, C) Images of representative seedlings at 14 DAS: (B) seedlings from control seeds; (C) seedlings from photooxidized seeds at 10 μmol m^{-2} s^{-1}. Abbreviations: co, cotyledon; fl, first leaves; lr, lateral root; pr, primary root. Scale: 2 mm.

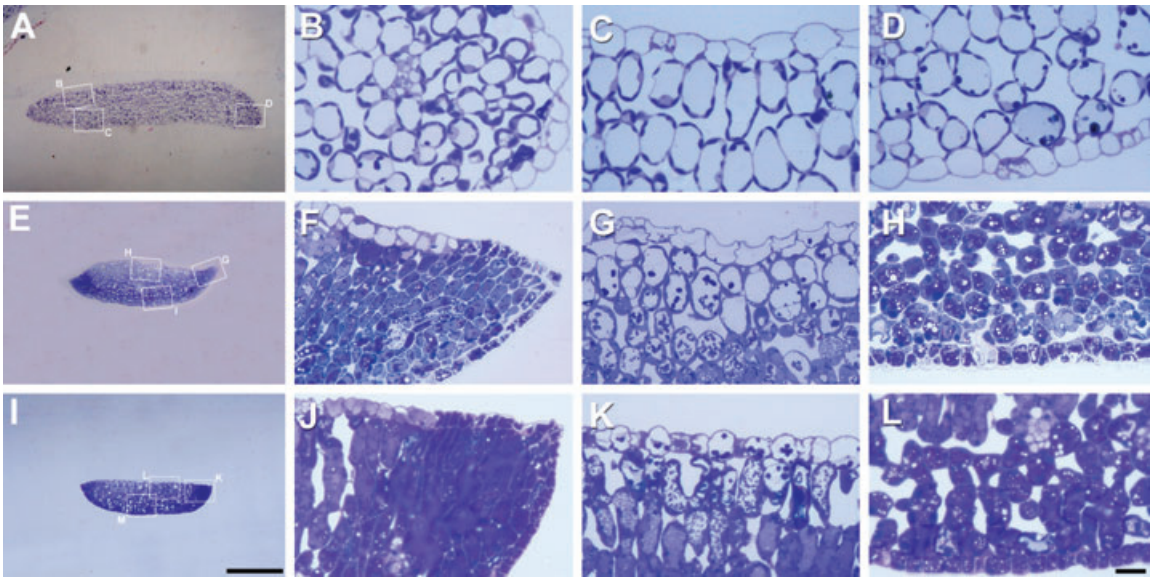

Fig. 2. Transverse sections of one cotyledon at 3 DAS. (A) control; (B–D) details of margin, adaxial side and abaxial side, respectively. (E) Cotyledon of a seedling derived from seed photooxidized at 2 μmol m^{-2} s^{-1}; (F–H) details of margin, adaxial side and abaxial side, respectively. (I) Cotyledon of a seedling from seed photooxidized at 10 μmol m^{-2} s^{-1}; (J–L) details of margin, adaxial side and abaxial side, respectively. The images are representative of at least 10 sections of cotyledons from different seedlings, from three independent treatments. Scale: 300 μm (A, E, I). Details: 150 μm.

a single, large central vacuole (Fig. 2A–D). Then, the cytoplasm containing a nucleus and other organelles was displaced to the periphery (Fig. 2A–D).The formation of a central vacuole is associated with cellular expansion. At the same stage, well-developed cristae were visible in mitochondria and chloroplasts were elliptical and contained starch grains (Fig. 3A), Mitochondria, rough endoplasmic reticulum, ribosomes and dictiosomes were frequent, indicating a very active metabolism.

The seedlings generated from photooxidized seeds revealed visible damage (Fig. 2E–L), especially in the abaxial epidermis and its subjacent tissues (Fig. 2H, L), and in cotyledon margins (Fig. 2F, J). In these sites, cells did not consume the storage reserves and, consequently, did not expand (Fig. 3B–D). The cotyledon margins showed reduced (Fig. 2F) or no (Fig. 2J) intercellular spaces.

On the contrary, in the abaxial mesophyll, intercellular spaces were visible (Fig. 2H–L). Cells in an intermediate stage, with partially consumed reserves, were also observed. Cotyledons differed in the number of layers strongly affected, from five layers in those originated from seeds exposed to 2 μmol m^{-2} s^{-1} (Fig. 2H) to eight in seedlings from seeds photooxidized at the highest light intensity (Fig. 2L).

Although cells in the adaxial mesophyll also revealed damage, they still consumed their reserves, differentiated organelles and expanded, though to a significantly lesser extent than the controls (Fig. 2G, K). In these cells, chloroplasts were abnormal, exhibiting a spherical shape, unilaterally displaced grana, abundant stroma and numerous plastoglobuli (Fig. 3E, F). Mitochondria were apparently not affected (Fig 3G, H). Following germination, cells of the adaxial mesophyll almost immediately began active autophagy, as seen by organelles embedded in the vacuole (Fig. 3G) at different stages of digestion. Multivesicular bodies were also abundant, revealing active endocytosis. In fact, multivesicular bodies were formed by pinching off from the plasma membrane, before passing through the cytoplasm and finally being taken up by the vacuole (Fig. 3G–I).

ROS production

In cotyledons of photooxidized seeds, an active $O_2^{\bullet-}$ production could be detected soon after imbibition, and continued during the whole experimental period (Fig. 4). $O_2^{\bullet-}$ radical formation was particularly high in seedlings from the 10 μmol m^{-2} s^{-1}photooxidation treatment, where NBT stained most of the cotyledon surface (Fig. 4B). $O_2^{\bullet-}$ production was also detected in the radical apexes and lateral roots, and in the vascular cylinder of the hypocotyls. In control seedlings, active $O_2^{\bullet-}$ generation was mostly restricted to the root apex, and, to a lesser extent, to the vascular cylinder of the

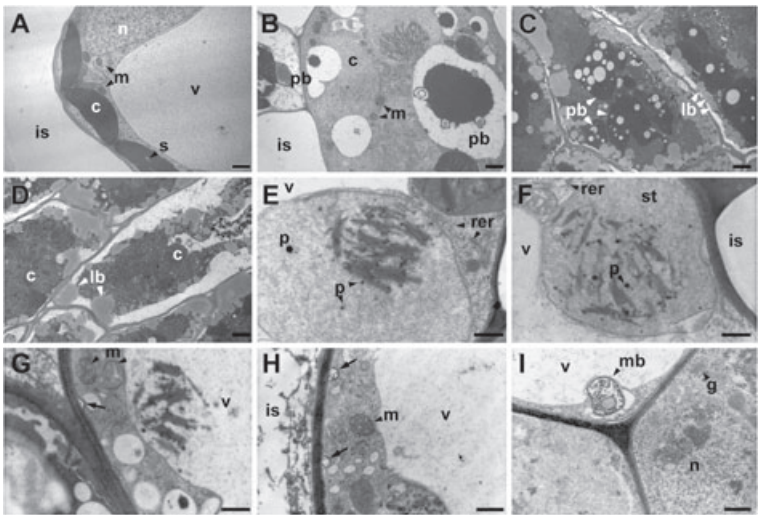

Fig. 3. Ultrathin sections of cotyledons from *Salix nigra* L. seedlings at 3 DAS. (A) Control seedling, adaxial tissue. (B–D) Seedling derived from seeds photooxidized at 2 μmol m^{-2} s^{-1}. (B) Abaxial tissue; (C, D) marginal tissue; in (B), partially consumed proteins from protein bodies and formation of intercellular spaces; in (C) and (D), cells were unable to consume their reserves, and protein and lipid bodies persisted but in (D), the central vacuole had begun to develop and the cell is plasmolyzed; (E–I) adaxial tissue of a cotyledon from the 10 μmol m^{-2} s^{-1} photooxidation treatment; (E, F) details of a cell, with mitochondria and chloroplasts; chloroplasts exhibited expanded stroma, plastoglobuli and disorganized grana; (G) a chloroplast is being autophagocyted in a vacuole; (G–I) multivesicular bodies are shown: in (G, H), originating from the plasmalemma (arrows). In (I), a multivesicular body right before being taken up by the central vacuole. Abbreviations: c, chloroplast; g, golgi apparatus; is, intercellular space; lb, lipid body; m, mitochondrion; mb, multivesicular body; n, nucleus; p, plastoglobuli; pb, protein body; rer, rough endoplasmic reticulum; s, starch; st, stroma; v, vacuole. Scale (A–E) 4 μm; (F–J) 3 μm.

root, consistent with previously reported data for this species (Causin et al. 2012, Roqueiro et al. 2012).

The formation of H_2O_2 as revealed by DAB treatment was very low and did not show a clear pattern among the different treatments (data not shown).

Lipid peroxidation and antioxidant enzyme activity

When seeds were photooxidized with low light intensity, MDA concentration increased, reaching a peak at 3 DAS. MDA levels subsequently decreased, reaching values similar to the control at 14 DAS (Fig. 5). When seeds were photooxidized with 10 μmol m^{-2} s^{-1}, MDA concentration increased about fivefold during the first 7 DAS, and remained high throughout the rest of the experimental period.

At 0 DAS, the activity of all antioxidant enzymes analyzed was lower than the control in seedlings from both photooxidation treatments (Fig. 6). In seedlings derived from the low light treatment, the activity of POX, CAT and APX markedly increased with time and reached maximum values at either 7 or 14 DAS, depending on the enzyme. A similar trend was observed in seedlings from the high light treatment, although APX (Fig. 6B) and CAT (Fig. 6D) levels did not exceed those of their respective controls. On the contrary, SOD activity remained at a level similar to (low light treatment) or significantly lower than (high light treatment) the control during most of the experimental period. (Fig. 6C).

Discussion

During germination in photooxidized *S. nigra* seeds, structural damage in tissues was observed on the abaxial side of cotyledons. The number of cell layers affected, i.e. the depth of the structural damage, depended on the intensity of the light treatment, reaching 5 when 2 μmol m^{-2} s^{-1} were used and 8 at 10 μmol m^{-2} s^{-1}. In both cases, the damage to the abaxial layers turned out to be irreversible because the cells affected lost their capacity for differentiation and, consequently, could not expand. This explains why the seedlings from photooxidized seeds have smaller cotyledons than the controls. Furthermore, despite consuming their reserves differentiating organelles and expanding, cells from the adaxial side of cotyledons were still smaller than equivalent cells in control seedlings.

These results are consistent with those recently obtained by Taleisnik et al. (2009) in a study with leaves from grasses, which reports that the decrease in foliar expansion is an effect shared by different types of abiotic stress. According to the authors (Taleisnik et al. 2009 and the works cited therein), both the signaling mediated by

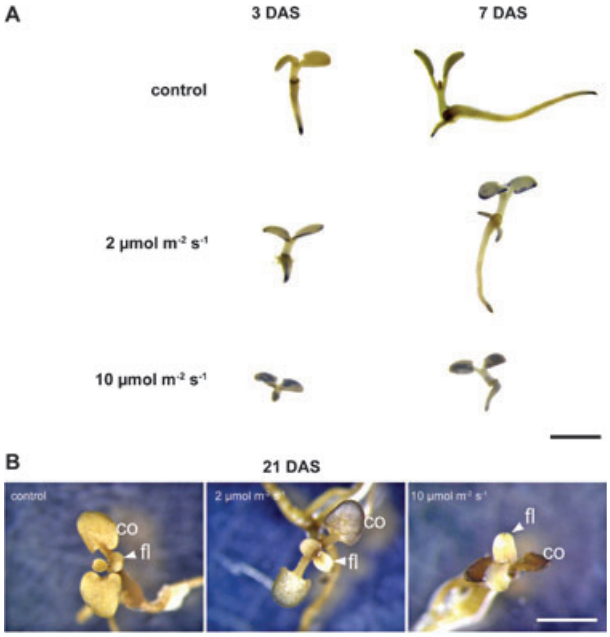

Fig. 4. $O_2^{\bullet-}$ production during morphogenesis: seedlings derived from control seeds and seeds photooxidized for 3 days at 2 or 10 µmol m^{-2} s^{-1} were monitored following NBT staining. (A) 3 DAS and 7 DAS seedlings vary greatly from control to 10 µmol m^{-2} s^{-1}, with reductions in development and increases in NBT staining. (B) Detail of shoot apices at 21 DAS, with clear differences in: (1) development of first leaves; (2) cotyledon expansion; (3) NBT staining in cotyledons. Note that NBT staining did not affect the first leaves in any treatment. Abbreviations: co, cotyledon; fl, first leaves. In (A), scale 0.25 mm; in (B), scale 2 mm.

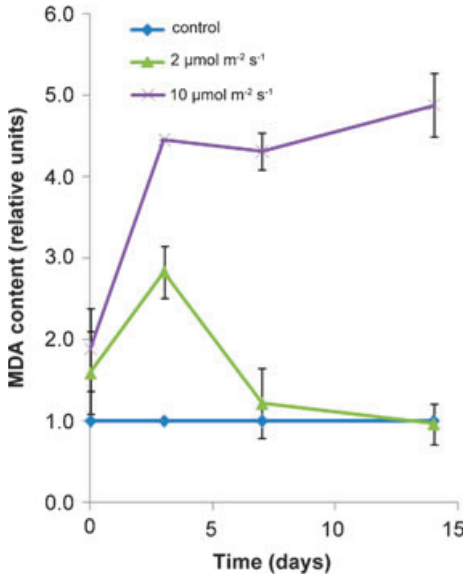

Fig. 5. MDA content in seeds photooxidized at 2 or 10 µmol m^{-2} s^{-1}, and in the respective seedlings at 3, 7 and 14 DAS. Results are expressed as relative units with respect to the MDA levels in non-photooxidized controls.

certain hormones and variations in ROS levels may play a central role in the development of this response.

Under MET examination, the cells of the adaxial layers (that apparently were non-affected) exhibited normal mitochondria but anomalous chloroplasts. The main damages observed in chloroplasts were similar to those found in leaves of different species exposed to different types of abiotic stress (Gabara et al. 2003, Wi et al. 2005, Xu et al. 2006, Chen et al. 2011, Zhang et al. 2011). These included: disruption of the chloroplast membrane, distortion of chloroplast shape, considerable increase in stromal area, reduced number of thylakoids per granum, disorganization of thylakoids and increased presence of plastoglobuli. According to Austin et al. (2006), plastoglobuli are lipoprotein particles that are found during the upregulation of plastid lipid metabolism either in response to oxidative stress or during cell death. Likewise, such changes in chloroplasts have already been reported in the dry tissues of photooxidized willow seeds (Roqueiro et al. 2010), suggesting that they may constitute a common response to abiotic stress in chloroplasts, regardless of the level of tissue hydration or stress type.

According to Van Breusegem and Dat (2006), both mitochondria and chloroplasts are major intracellular sources of ROS and hence may generate intermediate signals involved in programmed cell death (PCD) (Tanaka and Tanaka 2006). Under normal conditions, a series of antioxidant mechanisms regulates ROS formation in chloroplasts (Apel and Hirt 2004). When plants are exposed to diverse types of stress, this delicate balance is broken and the photochemical efficiency of the leaf is reduced due to ROS accumulation and oxidative damage (Bi et al. 2009). In willow seedlings derived from photooxidized seeds, production of the radical $O_2^{\bullet-}$ in cotyledons revealed a localization pattern similar to that of tissue damage. This is consistent with the presence of abnormal chloroplasts in the cells of the innermost tissues, suggesting that the production of this radical is closely related to the changes observed in them. Similar results were found in *Arabidopsis thaliana* exposed to different types of stress (Yao and Greenberg 2006, Bi et al. 2009). On the contrary, no significant amounts of H_2O_2 were found in any of the organs during the development stages following germination. This is consistent with the data reported by Roqueiro et al. (2012), and may be a consequence of the high stimulation of POX and (to a lesser extent) APX activities observed after the photooxidation treatments. It is worth noting that increments of peroxidase activity similar to those observed in this work have been reported in seedlings of other species exposed to different types of abiotic stress (Lee and Lin

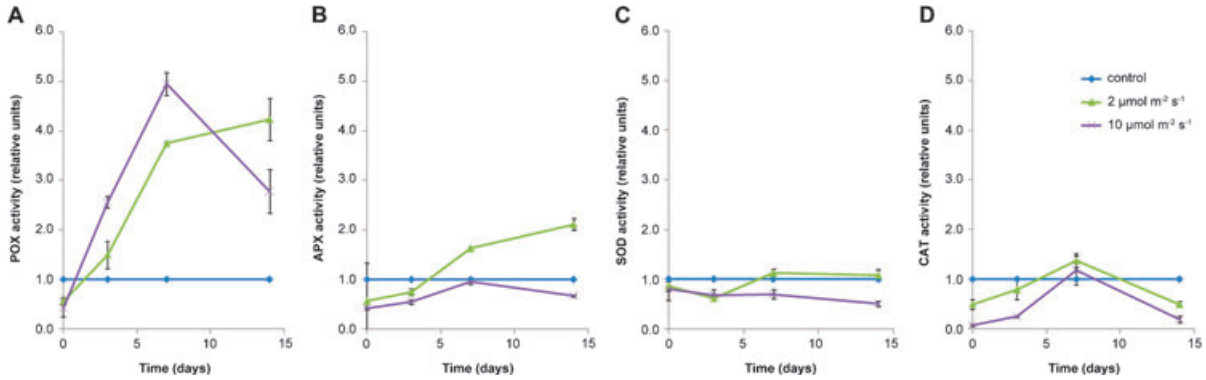

Fig. 6. (A) POX, (B) APX, (C) SOD, (D) CAT specific activities, in *Salix nigra* seeds photooxidized during 3 days at 2 or 10 µmol m^{-2} s^{-1}, and in the respective seedlings at 3, 7 and 14 DAS. Results are expressed as relative units with respect to the enzyme activities of non-photooxidized controls.

1995, Oidaira et al. 2000, Choi et al. 2004, Dey et al. 2007, Chugh et al. 2011). On the other hand, the lack of significant increases in H_2O_2 concentration might explain the low activation levels of CAT, as reported in pea (Yao et al. 2012) and tobacco (Willekens et al. 1997).

Several authors have shown that a high MDA content is an indicator of oxidative stress and tissue damage (McDonald 1999, Borsani et al. 2001, Singh et al. 2006). The present study demonstrated that: (1) in seedlings derived from seeds photooxidized at a low light intensity (2 µmol m^{-2} s^{-1}), the recovery that occurs in the period following germination was reflected by changes in MDA content: indeed, despite revealing a considerable increase during the first 3 DAS, MDA then rapidly fell until reaching values similar to the control; (2) in seedlings derived from photooxidized seeds at 10 µmol m^{-2} s^{-1}, MDA did not show any sign of recovery, which is consistent with the absence of morphogenesis and therefore the interruption in development.

In the adaxial tissues, numerous multivesicular bodies were seen deriving from the plasma membrane, before moving through the cytoplasm and finally being taken up by the vacuole. According to Staehelin and Newcomb (2000), multivesicular bodies are complex intracellular organelles that participate in exocytosis and endocytosis, during autophagy. A major function of the endocytic pathway is to sort internalized macromolecules and membrane proteins. These bodies arise by invagination of the limiting membrane of vesicles such that many small internal vesicles are formed. Additionally, expanded cells of the mesophyll of seedlings from photooxidized seeds exhibited a very early active cellular endocytosis and autophagy, both associated with the premature death of cotyledons. In this regard, Hu et al. (2012) identify PCD as a key mechanism that occurs during elm seeds under controlled deterioration treatment, suggesting an important role for PCD in seed deterioration.

With photooxidation structurally affecting the innermost tissues, including the shoot apical meristem, seeds lost their ability to develop the shoot and eventually did not survive regardless of seedling condition. Simultaneously, survival percentage was significantly reduced in seedlings grown from seeds photooxidized at 10 µmol m^{-2} s^{-1}. In contrast, when photooxidation was restricted to the outermost layers, TG percentage was similar to that of the control. Nonetheless the function of cotyledons was negatively affected, favoring the premature growth of the first leaves.

Conclusion

Early and active endocytosis, changes in chloroplast morphology, as well as the accumulation and diffusion of ROS play important roles in the early cell death of cotyledonary tissues in *Salix* seedlings from photooxidized seeds. Following germination, these seedlings can anticipate the emergence of first leaves, which would in turn complement the altered functionality of the damaged cotyledons. However, this switch is only possible if the antioxidant defense is not downregulated beyond a critical threshold, and if the shoot apical meristem has not been irreversibly damaged by ROS.

References

Aeibi H (1984) Catalase in vitro. Methods Enzymol 105: 121–126

Apel K, Hirt H (2004) Reactive oxygen species: metabolism, oxidative stress, and signal transduction. Annu Rev Plant Biol 55: 373–399

Arya SR, Bhagat S, Virendra-Singh I (1988) Preliminary studies on seed germination and viability of *Salix alba* and *Salix elegans*. Van Vigyan 26: 88–90

Austin JR II, Frost E, Vidi P-A, Kessler F, Staehelin A (2006) Plastoglobules are lipoprotein subcompartments of the chloroplast that are permanently coupled to thylakoid membranes and contain biosynthetic enzymes. Plant Cell 18: 1693–1703

Beauchamp C, Fridovich I (1971) Superoxide dismutase: improved assays and an assay applicable to acrylamide gels. Anal Biochem 44: 276–287

Bi Y, Chen W, Zhang W, Zhou Q, Yun L, Xing D (2009) Production of reactive oxygen species, impairment of photosynthetic function and dynamic changes in mitochondria are early events in cadmium induced cell death in *Arabidopsis thaliana*. Biol Cell 101: 629–643

Borsani O, Diaz P, Agius MF, Valpuesta V, Monza J (2001) Water stress generates an oxidative stress through the induction of a specific Cu/Zn superoxide dismutase in *Lotus corniculatus* leaves. Plant Sci 161: 757–763

Causin HF, Roqueiro G, Petrillo E, Láinez V, Pena LB, Marchetti CF, Gallego SM, Maldonado S (2012) The control of root growth by reactive oxygen species in *Salix nigra* Marsh. seedlings. Plant Sci 183: 197–205

Chen L, Han Y, Jiang H, Korpelainen H, Li C (2011) Nitrogen nutrient status induces sexual differences in responses to cadmium in *Populus yunnanensis*. J Exp Bot 62: 5037–5050

Choi DG, Yoo NH, Yu CY, de los Reyes B, Yun SJ (2004) The activities of antioxidant enzymes in response to oxidative stresses and hormones in paraquat-tolerant *Rehmannia glutinosa* plants. J Biochem Mol Biol 37: 618–624

Chugh V, Kaur N, Gupta AK (2011) Evaluation of oxidative stress tolerance in maize (*Zea mays* L.) seedlings in response to drought. Indian J Biochem Biophys 48: 47–53

Daws MI, Garwood NC, Pritchard HW (2006) Prediction of desiccation sensitivity in seeds of woody species: a probabilistic model based on two seed traits and 104 species. Ann Bot 97: 667–674

Dey SK, Dey J, Patra S, Pothal D (2007) Changes in the antioxidative enzyme activities and lipid peroxidation in wheat seedlings exposed to cadmium and lead stress. Braz J Plant Physiol 19: 53–60

Farrant JM, Pammenter NW, Berjak P (1992) Development of the recalcitrant (homoiohydrous) seeds of *Avicennia marina*: anatomical, ultrastructural and biochemical events associated with development from histodifferentiation to maturation. Ann Bot 70: 75–86

Farrant JM, Pammenter NW, Berjak P, Walters C (1997) Subcellular organization and metabolic activity during the development of seeds that attain different levels of desiccation tolerance. Seed Sci Res 7: 135–144

Gabara B, Sklodowska M, Wyrwicka A, Glińska S, Gapińska M (2003) Changes in the ultrastructure of chloroplasts and mitochondria and antioxidant enzyme activity in *Lycopersicon esculentum* Mill. leaves sprayed with acid rain. Plant Sci 164: 507–516

Hodges MD, De Long JM, Forney CF, Prange RK (1997) Improving the thiobarbituric acid-reactive-substances assay for estimating lipid peroxidation in plant tissues containing anthocyanin and other interfering compounds. Planta 207: 604–611

Hong TD, Linington S, Ellis RH (1996) Seed Storage Behaviour: A Compendium (Electronic Version). International Plant Genetic Resource Institute, Rome

Hu D, Ma G, Wang Q, Yao J, Wang Y, Pritchard HW, Wang X (2012) Spatial and temporal nature of reactive oxygen species production and programmed cell death in elm (*Ulmus pumila* L.) seeds during controlled deterioration. Plant Cell Environ 35: 2045–2059

Lee TM, Lin YH (1995) Changes in soluble and cell wall-bound peroxidase activities with growth in anoxia-treated rice (*Oryza sativa* L.) coleoptiles and roots. Plant Sci 106: 1–7

Leprince O (2003) Assessing desiccation sensitivity: from diagnosis to prognosis. In: Smith RD, Dickie JB, Linington SH, Pritchard HW, Probert RJ (eds) Seed Conservation: Turning Science into Practice. Kew Royal Botanic Gardens, Kew, pp 390–414

Marin L, Dengler RE (1972) Granal plastids in the cotyledons of the dry embryo of *Kochia childsii*. Can J Bot 50: 2049–2052

Maroder HL, Prego IA, Facciuto GR, Maldonado SB (2000) Storage behaviour of *Salix alba* and *Salix matsudana* seeds. Ann Bot 86: 1017–1021

Maroder HL, Prego IA, Maldonado SB (2003) Histochemical and ultrastructural studies on *Salix alba* and *Salix matsudana* seeds. Trees 17: 193–199

McDonald MB (1999) Seed deterioration: physiology, repair and assessment. Seed Sci Technol 27: 177–237

Nakano Y, Asada K (1987) Purification of ascorbate peroxidase in spinach chloroplasts: its inactivation in ascorbate-depleted medium and reactivation by monodehydroascorbate radical. Plant Cell Physiol 28: 131–140

Oidaira H, Sano S, Koshiba T, Ushimaru T (2000) Enhancement of antioxidative enzyme activities in chilled rice seedlings. J Plant Physiol 156: 811–813

Pammenter NW, Greggains V, Kioko JI, Wesley-Smith J, Berjak P, Finch-Savage WE (1998) Effects of differential drying rates on viability retention of recalcitrant seeds of *Ekebergia capensis*. Seed Sci Res 8: 463–471

Pinfield NJ, Stobart AK, Crawford RM, Beckett A (1973) Carbon assimilation by sycamore cotyledons during early seedling development. J Exp Bot 24: 1203–1207

Pólya L (1961) Injury by soaking of *Populus alba* seeds. Nature 4759: 159–160

Popova EV, Kim DH, Han SH, Pritchard HW, Lee JC (2012) Narrowing of the critical hydration window for cryopreservation of *Salix caprea* seeds following ageing and a reduction in vigour. Cryo Letters 33: 220–231
Prochazkova D, Sairam RK, Srivastava GC, Singh DV (2001) Oxidative stress and antioxidant activity as the basis of senescence in maize leaves. Plant Sci 161: 765–771
Romero-Puertas MC, Rodríguez-Serrano M, Corpas FJ, Gómez M, del Río LA, Sandalio LM (2004) Cadmium-induced subcellular accumulation of O_2^- and H_2O_2 in pea leaves. Plant Cell Environ 27: 1122–1134
Roqueiro G, Facorro GB, Huarte MG, Rubín de Celis E, García F, Maldonado S, Maroder H (2010) Effects of photooxidation on membrane integrity in *Salix nigra* seeds. Ann Bot 105: 1027–1034
Roqueiro G, Maldonado S, Ríos MC, Maroder H (2012) Fluctuation of oxidative stress indicators in *Salix nigra* seeds during priming. J Exp Bot 63: 3631–3642
Singh HP, Batish DR, Kaur S, Arora K, Kohli R (2006) α-pinene inhibits growth and induces oxidative stress in roots. Ann Bot 98: 1261–1269
Staehelin LA, Newcomb EH (2000) Membrane structure and membranous organelles. In: Buchanan BB, Gruissem W, Jones RL (eds) Biochemistry & Molecular Biology of Plants. American Society of Plant Physiologists, Rockville, pp 1–50
Taleisnik E, Rodríguez AA, Bustos D, Erdei L, Ortega L, Senn ME (2009) Leaf expansion in grasses under salt stress. J Plant Physiol 166: 1123–1140
Tanaka A, Tanaka R (2006) Chlorophyll metabolism. Curr Opin Plant Biol 9: 248–255
Teng SC, Yu H (1948) Propagation of weeping willow from seed. Bot Bull Acad Sin 2: 131–132
Van Breusegem F, Dat JF (2006) Reactive oxygen species in plant cell death. Plant Physiol 141: 384–390
Vavilin DV, Ducruet JM, Matorin DN, Venediktov PS, Rubin AB (1998) Membrane lipid peroxidation, cell viability and photosystem II activity in the green alga *Chlorella pyrenoidosa* subjected to various stress conditions. Photochem Photobiol 42: 233–239
Werker E (1997) Seed Anatomy. Gebrüder Borntraeger, Berlin
Wi S, Chung B, Kim JH, Baek MH, Yang D, Lee JW, Kim JS (2005) Ultrastructural changes of cell organelles in *Arabidopsis* stems after gamma irradiation. J Plant Biol 48: 195–200
Willekens H, Chamnongpol S, Davey M, Schraudner M, Langebartels C, van Montagu ID, Camp WV (1997) Catalase is a sink for H_2O_2 and is indispensable for stress defense in C_3 plants. EMBO J 16: 4806–4816
Xu S, Li J, Zhang X, Wei H, Cui L (2006) Effects of heat acclimation pretreatment on changes of membrane lipid peroxidation, antioxidant metabolites, and ultrastructure of chloroplasts in two cool-season turfgrass species under heat stress. Environ Exp Bot 56: 274–285
Yao N, Greenberg JT (2006) *Arabidopsis ACCELERATED CELL DEATH2* modulates programmed cell death. Plant Cell 18: 397–411
Yao Z, Liu L, Gao F, Rampitsch C, Reinecke DM, Ozga JA, Ayele BT (2012) Developmental and seed aging mediated regulation of antioxidative genes and differential expression of proteins during pre- and post-germinative phases in pea. J Plant Physiol 169: 1477–1488
Zhang S, Jiang H, Peng S, Korpelainen H, Li C (2011) Sex-related differences in morphological, physiological, and ultrastructural responses of *Populus cathayana* to chilling. J Exp Bot 62: 675–686
Zhukova GY, Yakovlev MS (1966) Electron microscope study of the chloroplasts of a *Nelumbo nucifera* Gaertn embryo (in Russian). Bot Zh Akad Nauk 51: 1542–1546

Edited by C. Foyer